

Volatile organic compound emission profiles of rural cooking and heating in Guanzhong Plain, China, and its potential effect on regional O₃ and secondary organic aerosol formation

Jian Sun^{1,2}, Zhenxing Shen^{1,2*}, Yu Huang², Junji Cao², Steven Sai Hang Ho^{2,3}, Xinyi Niu², Taobo Wang¹, Qian Zhang¹, Yali Lei¹, Hongmei Xu¹, Hongxia Liu¹

¹Department of Environmental Sciences and Engineering, Xi'an Jiaotong University, Xi'an, 710049, China

²Key Lab of Aerosol Chemistry & Physics, SKLLQG, Institute of Earth Environment, Chinese Academy of Sciences, Xi'an, 710049, China

³Division of Atmospheric Sciences, Desert Research Institute, Reno, NV 89512, United States

**Author to whom correspondence should be addressed. E-mail: zxshen@mail.xjtu.edu.cn (Zhenxing Shen).*

Abstract

Solid fuels (i.e., biomass fuel and coal) burned for cooking and heating emit large amounts of pollutants, including particulate matter (PM) and volatile organic compounds (VOCs), into the atmosphere. In this study, VOCs were directly collected in chimneys of residential cooking and heating stoves in the Guanzhong Plain using an adsorbent tube approach followed by thermal desorption-gas chromatography/mass spectrometry analysis. Emission factors (EFs) of targeted VOCs varied from 0.047 ± 0.019 to $3.12 \pm 1.59 \text{ g kg}^{-1}$ with a descending order of biomass straw > woody fuels >> coal fuels, although the differences between straw and woody fuels were not significant ($p > 0.05$). A remarkable finding is that semi-gasifier stoves could not suppress VOC emissions even though a high efficiency in reduction of PM was demonstrated. In addition, high values of coefficients of divergence (CDs) (most > 0.5) indicated that large variations existed in the VOC profiles for different fuels and stoves. Ozone formation potential (OFP) of VOCs from solid fuel burning ranged from 0.050 to 5.91 g kg^{-1} , contributing approximately 20% of the Guanzhong's ozone formation in winter. The values were much larger than the contribution from solid fuel burning to primary PM (6.7%). However, much lower secondary organic aerosol (SOA) formation potentials ($0.5\text{--}45.6 \text{ mg kg}^{-1}$) of VOCs emitted from solid fuel burning were estimated. The values were two orders of magnitude lower than OFP values and only accounted for 0.23% of the SOA in the Guanzhong. The results of this study demonstrated that the VOC emission from solid fuel burning had a strong impact on ozone pollution in the Guanzhong Plain during the heating season.

1. Introduction

Solid fuels (mainly biomass and coal) are extensively used for daily cooking and heating in developing countries, particularly in rural regions (Shen et al., 2013). Biomass burning is the largest contributor of fine carbonaceous particles and second largest source of trace gases in the global atmosphere (Akagi et al., 2011; Andreae et al., 2001). [More than 60% of households in rural China use traditional biomass resources as major fuels \(Hou et al., 2017\).](#) Additional contributions from coal burning should not be underestimated. However, because of the relatively low efficiencies of fuels burned in residential stoves, large quantities of incomplete combustion byproducts, such as fine particulate matter (PM) and volatile organic compounds (VOCs), are emitted (Adkins et al., 2010; Zhang and Smith, 2007).

Chemical profiles of PM emitted from residential burning of solid fuels have been widely studied (Bonjour et al., 2013; Lei et al., 2011; Winijkul and Bond, 2016). [Studies on trace gases, including VOCs, have been relatively rare \(Chagger et al., 1999; Chen et al., 2016; Evtyugina et al., 2014\), even though their effects on atmospheric pollution are comparable to that of PM \(Lee et al., 2005\).](#) VOCs participate in the formation of tropospheric ozone (O_3), other atmospheric oxidants, and secondary organic aerosols (SOA) in particulate phases (Duan et al., 2008; Liu et al., 2008). Primary VOC emission, along with the resulting photochemical oxidant and fine particle formation, can lead to severe regional air pollution and contribute to climate change (Langmann et al., 2009; Yuan et al., 2010). Because of diverse burning conditions, fuels, and apparatus (i.e., fuel and stove types), the emission factors (EFs) of VOCs vary widely among different regions or even among neighboring areas (Iinuma et al., 2010; Li et al., 2009; Reid et al., 2005).

The Guanzhong Plain, with an area of approximately 36,000 km² and population of 23.92 million, is surrounded by the Qinling Mountains to the south and the Loess Plateau to the north (Figure S1); atmospheric dispersion is typically weak due to the unique features of its topography (Niu et al., 2016). Hou et al. (2017) reported that solid fuel burning accounts for >80% of the energy consumption of the Guanzhong Plain and is crucial in haze and episode events during winter (Cao et al., 2005; Shen et al., 2009; Zhang et al., 2015). PM emitted from rural cooking and heating activities exerts substantial effects in the Guanzhong Plain and these effects have been well studied.

[In this paper, we particularly focus on the VOC emissions from solid fuel burning in the Guanzhong Plain. A measurement campaign was conducted in its rural environments to determine the EFs of VOCs from rural solid fuel burning activities and their contributions to regional \$O_3\$ and SOA formation.](#)

2. Methodology

2.1 Sample Collection

[VOC samples were collected at three typical agricultural villages in the rural Guanzhong Plain \(Fig. S1\) in winter 2014. The sampling campaign lasted for 3 weeks; each week was devoted to one sampling site. The village near Weinan city \(V1\) has the highest number of residents \(~2000\). Apple trees are the dominant crop; apple wood branches and logs are often used as fuels in the region's traditional stove—the Heated Kang stove \(Fig. S2a\). In the village near Xianyang city \(V2\), residents mainly use coal and wood branches for household heating and cooking, respectively. The village near](#)

Baoji city (V3) is located at a core grain-producing area in the Guanzhong Plain; here, maize straw and wheat straw are used for both heating and cooking in Heated Kang stoves. Table S1 summarizes detailed information on the solid fuels and stoves. Three types of stoves are mainly used: Heated Kang stoves, traditional coal heating stoves (Fig S2b), and semi-gasifier stoves (Fig. S2c). The characteristics of Heated Kang stoves was described in our previous study (Sun et al., 2017). Traditional coal heating stoves have simple iron structures and are commonly used heating devices in Northern China. Fuels (e.g. anthracite) are combusted in the furnace chambers and heat is transferred with low efficiencies by heat conduction or thermal radiation. Semi-gasifier stoves are based on a core technology called “secondary air supply”, which enhances combustion efficiency and reduces PM EFs (Sun et al., 2017). In total, eight solid fuel types were considered in this study: firewood, branches, maize straw, wheat straw, corncobs, anthracite, honeycomb fuel, and bitumite. These solid fuels were representative in the rural Guanzhong.

Insert Table S1

All VOC samples were collected in field experiments. The sampling platform was deployed on each rooftop and beside the chimney of each stove. A self-made dilution system with dilution rates from 5- to 50-fold was employed to collect the smoke emitted from solid fuel combustion. The control of dilution rate was realized by a multi-pump system, and the real-time flow of each pinch point was measured by flowmeters (TSI 4140, TSI, MN, USA). The smoke inlet of the dilution system was set perpendicular to the smoke plume and 0.1 m above the chimney. In our tests, the PM weight differences between different sampling channels were <5%, and the repeatability of dilution was >80% for field tests. More information on the dilution system was published in our previous study (Sun et al., 2017). Experiments were conducted while residents used the stoves and solid fuels in the course of their daily lives. For cooking, fuels were weighed using a balance with a precision of 0.1 g before and after burning to clear the net fuel consumption, and the sampling period covered the whole cooking process. For heating activities, we weighed the fuels every time they were added into each stove and each sampling period covered several cycles to account for the different combustion durations of fuels in various stoves. Six parallel diluted smoke channels were set—one for VOCs, three for PM_{2.5}, and two for online monitoring (CO and NO_x). For VOC sampling, an air stream of diluted smoke was drawn into a ¼” o.d. stainless steel multi-bed adsorbent tube filled with Tenax-TA, Carbograph I TD and Carboxen 1003 (Markes International Ltd., Llantrisant, UK) by a low-flow modular pump (ACTI-VOC, Markes International Ltd.) at a flow rate of 50 mL min⁻¹ for 30–60 min to account for different VOC concentrations. A Teflon filter assembly (47 mm, Whatman, Clifton, NJ, USA) and a self-made ozone scrubber [manufactured from a saturated potassium iodide (KI)-coated copper tube (length, 1 m; outer diameter, 0.25 inch)] were installed in the air upstream to remove any influences from PM and O₃, respectively. The sorbent tubes were pre-cleaned in a thermal conditioner (TC-20, Markes International Ltd.) at 330 °C for 20 min. All pre-conditioned and sampled tubes were capped and shipped at 0 °C. Nonsignificant breakthrough (<5%) was observed either in field or laboratory demonstration under this sampling flow and volume (Ho et al., 2017). Two sorbent tube samples were thus collected in each test, and one field blank was collected for each sampling campaign.

2.2 Chemical Analysis

In total, 27 valid sorbent tube samples were collected. The samples were analyzed using a thermal desorption (TD) unit (Series 2 UNITY-xr system, Markes International Ltd.) coupled with a gas chromatograph/mass spectrometric detector (GC/MSD; Model 7890A/5977B, Agilent, Santa Clara, CA, USA). A tube was connected into the TD unit at room temperature (~25°C) and purged with ultra-high purity helium (He) gas at a flow rate of 40 mL min⁻¹ for 10 s to eliminate air and oxygen intrusion. For the primary desorption stage, the analytes were desorbed at 330°C for 5 min and refocused onto a cryogenic-trap (U-T1703P-2S, Markes International Ltd.) to capture high volatility target compounds at -15°C. For the secondary desorption stage, the trap was dry-purged for 10 s, rapidly heated from -15°C to 320°C, and maintained for 5 min. The analytes were passed through a heated transfer line at 160°C, and re-refocused onto a cold GC capillary column head (Rtx-1, 105-mm × 0.25-mm × 1-μm-film thickness, Restek Corporation, Bellefonte, PA, USA) at -45°C by using liquid nitrogen (N₂) in a GC oven. After completing the second desorption, the oven temperature program started at an initial temperature of -45°C for 4 min, ramped to 230°C at a rate of 6°C min⁻¹, and was maintained at 230°C for 5 min. The constant flow rate of He carrier gas was 1.0 mL min⁻¹ throughout the GC analysis. The MSD was operated in selective ion monitoring mode at 230°C and at 70 eV for electron ionization. Identification was achieved by comparing the mass spectra and retention times of the chromatographic peaks with those of authentic standards. Certified PAMS (Photochemical Assessment Monitoring Stations) standard mixtures (Restek Corporation) were used in calibrations. A multi-point calibration curve was established to quantify each of the target compounds with linearity > 0.999. The minimum detection limits (MDLs) for 98 target analytes were in the range of 0.001–0.159 ppbv with a sampling volume of 3 L; the MDLs for all VOC species are listed in Table S2. The measurement precision levels for the analysis of eight replicates of standard samples at 2 ppbv were ≤5%. Duplicate samples were collected and the reproducibility was >95%. Background samples of VOCs were also collected and analyzed using the same protocol as that of source sample collection. The background concentrations of VOCs were subtracted off when calculating EFs and the data are listed in Table S3. Additional details on sampling and analytical methods have been published by Ho et al. (2017) and (2018).

Insert Tables S2 and S3

2.3 Data Processing

1) Emission factor calculations

EFs were calculated based on fuel weight consumption (g kg⁻¹) as

$$EF = \frac{m_{tube} \times DR \times t_{sample} \times V_{stk} \times D}{Q_{tube} \times m_{fuel}}, (1)$$

where m_{tube} is the mass of VOC in the adsorbent tube (mg), DR dilution ratio, t_{sample} sampling duration (s), V_{stk} stack flow velocity (m s⁻¹), D stack cross section area of chimney (m²), Q_{tube} sampling volume through the adsorbent tube (m³), and m_{fuel} fuel consumption (kg). The concentration data of VOCs used in EF calculations are listed in Table S4. The source and discussion of uncertainties are discussed in section 3.5.

Insert Table S4

2) Average and standard deviation calculation

For EFs, O₃ formation potential (OFP), SOA formation potential (SOAP), and other data are presented with error bars as average and standard deviation (SD) values. The average and SD were calculated as

$$\text{Average } (\mu) = \frac{\sum_{i=1}^N X_i}{N}, (2)$$

where X_i is the value of sample No. i and N the total sample number; and

$$\text{SD} = \sqrt{\frac{1}{N} \sum_{i=1}^N (x_i - \mu)^2}, (3)$$

where X_i is the value of sample No. i , N the total sample number, and μ the average of X_i .

3) Uncertainties

For VOC measurement, when the concentration is over the MDL, the uncertainties can be calculated as

$$\text{Uncertainties} = \sqrt{(\text{Error fraction} \times \text{Concentration})^2 + (0.5 \times \text{MDL})^2}, (4)$$

where error fraction is the error fraction in measurements, concentration is the measured concentration of VOC species, and MDL is the MDL for the corresponding VOC species.

When the concentration measured is below the MDL, the uncertainties should be calculated as

$$\text{Uncertainties} = \frac{5}{6} \times \text{MDL}. (5)$$

For uncertainties derived from multiple sources, the calculation should be the combination of uncertainties as

$$\text{Uncertainties} = \sqrt{\sum (\text{Unc}_i)^2}, (6)$$

where Unc_i denotes the uncertainties in different sources i .

3. Results and Discussion

3.1 EFs

EFs of eight VOC classes for the examined solid fuels are summarized in Table 1 (with detailed VOC profiles in Table S5). On average, the EFs for biomass fuels (1.12 ± 0.18 to $3.12 \pm 1.59 \text{ g kg}^{-1}$) were higher than those for coal fuels (0.047 ± 0.019 to $1.00 \pm 0.47 \text{ g kg}^{-1}$; $P < 0.05$). Among the biomass fuels, the EFs were in the following descending order: corncob > branch > firewood > maize straw > wheat straw. Our measured EFs were within the ranges reported for the biomass fuels shown in other relevant studies (Li et al., 2009; Wang et al., 2014). Our observations support that stoves and burning modes were the dominant factors affecting the EFs (Li et al., 2009). First, wheat straw and maize straw emitted more halogen-containing VOCs (0.093 ± 0.023 and $0.31 \pm 0.13 \text{ g kg}^{-1}$, respectively) than did firewood and branches (i.e., woody fuels; 0.045 ± 0.005 and $0.040 \pm 0.012 \text{ g kg}^{-1}$, respectively) in Heated Kang stoves ($P < 0.05$). This can be ascribed to the features of biomass straw fuels, which have higher chloride contents than do woody fuels (Lindberg et al., 2016). Second, marked differences in EFs were seen between the types of stoves used. The EFs of total quantified VOCs for branches with Heated Kang and semi-gasifier stoves were 1.83 ± 0.33 and $2.37 \pm 0.82 \text{ g kg}^{-1}$, respectively. The higher value from semi-gasifier stoves was contributed by increased aromatic hydrocarbon generation at relatively high combustion temperatures (Chen et al., 2016; Lemieux et al., 2004). Although some studies have demonstrated that semi-gasifier stoves can effectively reduce

particulate emissions (Acosta et al., 2011; Shen et al., 2015; Sun et al., 2017), the elevated VOC emissions remain a concern. Finally, burning mode (i.e., uses of either heating or cooking) also has strong effects on EFs. Heated Kang stove users often extend the burning process by shutting down the air supply, leading to an oxygen-deficient environment (Zhuang et al., 2009). This extremely oxygen-deficient condition increases production of unsaturated alkenes but produces little alcohol, relative to the use of traditional cooking stoves. However, a sufficient air supply may not be a panacea to reduce VOC emissions. The EFs of non-methane hydrocarbons from wheat straw fuels with open burning are more than 100% greater than those reported in this study (Lemieux et al., 2004; Li et al., 2009).

Insert Table 1 & Table S5

Table 2 shows the top 10 individual compounds with the highest contributions to the EFs of the total quantified VOCs in each test. Acetone, which accounted for 10% of the EFs for the biomass fuels, is one of the dominant VOCs regardless of stove type. For the emissions from Heated Kang stoves, the fractions of oxygenated-VOCs (O-VOCs) (27.2% to 31.2%) were also much higher than those of other stoves (6.6% to 23.1%). This could be explained by the severely oxygen-deficient conditions during straw fuel combustion when the volatile components could not be oxidized completely (Wang et al., 2014). Benzene and toluene were two most abundant aromatic compounds. The sum of their contributions was in the following descending order: semi-gasifier stove > cooking stove > Heated Kang stove. The generation of aromatic hydrocarbons demonstrated a positive correlation with increases in combustion temperatures (Shen et al., 2015). Because semi-gasifier and traditional cooking stoves had sufficient air supplies, they formed large quantities of aromatic hydrocarbons. Methyl chloride was the sole halogen-containing compound in the top 10 series of all tests. It acts as a typical tracer for straw burning (Liu et al., 2008) and is crucial in source identification (Wang et al., 2014). Among most profiles, iso-pentane is listed in the top 10 species; however, it is mainly derived from vehicle emission (Hwa et al., 2002; Liu et al., 2008). Contamination by vehicle emission at such a large scale in combustion emission sampling was hardly possible. Therefore, the mechanism of high emission of iso-pentane should be researched in subsequent studies.

Insert Table 2

Alkane is the most abundant class of emissions from the combustion of anthracite and honeycomb coal fuels. Dodecane and *n*-butane were the two most dominant alkanes for anthracite (26.6%) and honeycomb (29.2%) fuels burned in cooking stoves. For anthracite burned in semi-gasifier stoves, dodecane also accounted for 21.2% of the total quantified alkanes. Bitumite had a different VOC emission profile, which resembled a mix between the profiles of woody fuel and anthracite coal fuel. Aromatic hydrocarbons (i.e., benzene, toluene, and naphthalene) were the top ten species for bitumite with an average contribution of 25.2%, which resembled the loadings of woody fuels in semi-gasifier stoves. However, alkanes, including dodecane, *n*-butane, undecane, iso-butane, propane, iso-pentane

and n-pentane, for bitumite burning still had a high contribution of 37.6% to total quantified VOCs, which was consistent with that for anthracite (Liu et al., 2008). The small variations between the two fuels could be ascribed to their similarities of fuel properties such as ash content and fixed carbon fractions.

3.2 Source Profiles

Figure S3 illustrates the source profile for each test in this study. The identity numbers of each VOC are given in Table S5. Among those woody fuels (Fig. S3a), four characteristic fractions are shown, including C₃-C₅ alkanes, C₃ alkene, benzene and toluene, and C₃-C₄ carbonyls (i.e., acrolein, acetone, and methyl ethyl ketone). Coefficient of divergence (CD) was calculated to measure the similarity of profiles between the tests (Table S6). Similar profiles were obtained with the same stoves (CD = 0.23 for Heated Kang, and CD = 0.35 for semi-gasifier stoves), which can be compared with much higher CD values (> 0.5) between different stoves. The main difference between the Heated Kang and semi-gasifier stove profiles were aromatic hydrocarbons, particularly benzene and toluene.

Insert Figure S3

Insert Tables S6

Regarding the burning of coal fuels, two additional characteristic fractions, namely ethanol and dichlorobenzene (including three isomers), were seen in their VOC profiles. Moreover, their proportions of halogen-containing compounds were obviously higher than those of woody fuels. This phenomenon has been observed by (Chagger et al., 1999; Liu et al., 2017); it is attributable to the rich chlorine content of coal (Vassilev et al., 2000; Yudovich and Ketris, 2006). In addition, the combustion of woody fuels emitted large proportions of alkenes (mainly propylene) whereas coal combustion emitted more C₁₁-C₁₂ alkanes (i.e., dodecanes and undecanes). Dodecane is the most abundant VOC from the combustion of four types of coals (as presented in Table 2). The CD values of bitumite-SG (i.e., bitumite burned in a semi-gasifier stove) vs. branch-SG/firewood-SG (0.46/0.47) are lower than those for anthracite-SG vs. branch-SG/firewood-SG (0.58/0.61); thus, VOC emissions from bitumite are more similar to those of woody fuels than to those of anthracite. The same result was also reported in Wang et al. (2014), in which the EFs of VOCs had good correlations with the calorific values and volatile matter (VM) percentages of fuels. In our study, the VM percentages of anthracite, bitumite, and firewood were 6.12%, 33.20%, and 82.96%, respectively (as listed in Table S7), and the calorific values of bitumite and firewood were close as well.

Insert Table S7

Among the coal fuels, anthracite fuel in semi-gasifier stoves and honeycomb fuel in cooking stoves showed the highest similarity (CD = 0.32) because the honeycomb briquettes used in this study were made of anthracite mixed with some additives. As with woody fuel, coal combustion in semi-gasifier stoves tended to produce considerable quantities of aromatic hydrocarbons. However, semi-gasifier stoves emitted smaller quantities of halogen-containing compounds than did traditional

coal stoves. The differences between combustion phenomena could affect the distributions of chlorine in solid and vapor phases (Westberg et al., 2003).

For the straw group (Fig.S3c), high CD values for the four characteristic fractions were shown between the woody fuel emissions. However, their emissions of halogen-containing compounds greatly resembled those for coal fuels because both biomass straw and coal fuels are rich in chlorine (Baxter, 2005). Table S6 also indicates that highly similar VOC profiles could be obtained with the same types of stoves (CD = 0.52 and 0.45) than with different types of stoves (CD = 0.71–0.84) even if different solid fuels were used. The VOC profiles for traditional cooking and semi-gasifier stoves had low CD values (0.44 and 0.49, respectively) because they were both operated in oxygen-rich burning modes. This can be further supported by the fact that the VOC profiles could be affected by fuel types, stove types, and burning modes. Notable differences (CD = 0.57) can be observed for the same fuels and stove types (branch and traditional stove) with different burning modes (heating or cooking).

3.3 OFP

Many VOCs are well known O₃ precursors in the atmosphere (Ho et al., 2013; Wang et al., 2017). To assess the photochemical reactivity of VOCs emitted from the combustion of solid fuels, two methods were applied to evaluate the contributions of individual VOCs to O₃ production. The first method was maximum incremental reactivity (MIR) method (Carter, 2009), which can be expressed as

$$\text{OFP} = [\text{VOC}_i] \times \text{MIR}_i, \quad (7)$$

where OFP is the ozone formation potential and VOC_i and MIR_i are the concentration and maximum incremental reactivity of some individual VOC_i, respectively. In Carter's study, the MIR model required a VOC-limited and high NO_x condition which applied to the Guanzhong area (Li et al., 2017; Xue et al., 2017; Zhang et al., 2015). The second method was propene-equivalent (Prop-Equiv) concentration (Atkinson and Arey, 2003), calculated as

$$\text{Prop-Equiv}_i = [\text{VOC}]_i \times k_{\text{OH},i}/k_{\text{OH,propene}}, \quad (8)$$

where K_{OH,i} and K_{OH,propene} are the rate constants of NMHCs reacted with OH at 298 K (cm³ molecule⁻¹ s⁻¹).

The averages and standard errors of OFPs and Prop-Equivalents are given in Figure 1a and 1b, respectively. The total OFPs for solid biomass fuels are higher than those for coal fuels. The highest of total OFPs was 5.91 g kg⁻¹—noted for firewood burned in Heated Kang stoves. Among those burning activities with Heated Kang stoves, alkenes were the major contributors that formed at an oxygen-deficient combustion condition. Higher OFP contributions from aromatic hydrocarbons were seen for semi-gasifier stoves, because aromatic hydrocarbons were produced abundantly from semi-gasifier stoves. Alkanes showed relatively low contributions to the total OFP for most fuels except anthracite because of their relatively low MIRs (Duan et al., 2008), even though the concentrations of iso-pentane and dodecane were high. For the calculated Prop-Equiv (Figure 1b), the contributions from each organic group were similar to the results of OFP. An obvious difference was that alkanes contributed higher fractions of the weight of Prop-Equiv, especially for cooking and coal fuel emissions. Even though long-chain alkanes have relatively high k_{OH} values (Carter, 2012), their reactivity toward O₃ formation through photochemical reactions is comparatively nonsignificant. As a result, the

Prop-Equiv method might reasonably over-estimate the contributions of alkanes to O₃ formation, especially for the VOC sources with high percentages of long-chain alkanes.

Insert Figure 1a and 1b

The total OFPs were generally lower for coal burning than biomass burning. The lowest OFP of 0.050 ± 0.019 g kg⁻¹ noted for honeycomb-CS (i.e., honeycomb fuel burned in a coal stove). Traditional coal stoves, due to their low operation temperatures and moderate combustion conditions, had the lowest OFPs in the tests; their OFPs were two orders of magnitude lower than those for woody fuels. Aromatic hydrocarbons contributed the majority of total OFP (~50%) from the coal stoves. Compared with the biomass fuels, the OFPs of the non-classified organic group, labeled as “other”, were much lower for coal burning, which was consistent with the results obtained by Liu et al. (2008). Bitumite is a mix of high VM fuels; its burning can lead to the formation of VOCs with the highest OFP among the four types of coal fuels. Aside from fuel features, semi-gasifier stoves also contributed to the high OFP for bitumite-SG. The OFP of anthracite-SG (0.62 ± 0.14 g kg⁻¹) was eight times higher than that of anthracite-CS (0.088 ± 0.003 g kg⁻¹) when anthracite was applied for both fuel tests ($p < 0.05$). No statistical difference ($p > 0.05$) between OFP for firewood-SG (5.74 ± 0.21 g kg⁻¹) and firewood-HK (5.91 ± 1.34 g kg⁻¹) was noted, demonstrating that semi-gasifier stoves could not suppress the potential O₃ formation in comparison of Heated Kang stoves. Thus, although they can limit PM emission, the semi-gasifier stoves are inefficient in limiting VOC emission and OFP (Shen et al., 2013; Sun et al., 2017).

An evaluation of O₃ contribution from solid fuel burning in the Guanzhong Basin was conducted and all parameters and results are listed in Table S8. The calculation method was presented in Tie et al. (2015) and Niu et al. (2016). We refined the box model and atmospheric capacity methods, and applied the hypothesis that the atmosphere would update every 24 h due to wind speed (Sun et al., 2017; Tie et al., 2015). From Table S8, the emission rate of OFP from biomass fuels (7.17 × 10⁴ kg day⁻¹) was approximately five times higher than that from coal fuels (1.55 × 10⁴ kg day⁻¹), provided that the annual consumption values of two types of fuels were at the same level. In addition, from our calculations, we estimated that the contribution of solid fuel burning to the O₃ production in the Guanzhong Basin in winter of 2013 was approximately 20% (OFP emission rate/O₃ atmospheric capacity). The value was much higher than that estimated with source apportionment approach with PM_{2.5} of 7.6% (Huang et al., 2014). Similar phenomena have been noted in other regions of China. For instance, biomass burning contributed to 6.7% and 4.8% PM_{2.5} (Huang et al., 2014) and 17.7% and 9.0% VOCs (Yuan et al., 2010) in Guangzhou and Shanghai, respectively. Thus, solid fuel burning contributed more toward VOC emissions than toward PM production in the Guanzhong Basin’s atmospheric environment.

Insert Table S8

3.4 SOAP

VOCs may be crucial precursors for SOA formation (Ho et al., 2017; Iinuma et al., 2010). Solid fuel combustion VOC contributions of photochemical reactivity to SOA formation were therefore estimated. Firstly, we adopted a Toluene-Equivalent method to calculate the SOAP of VOCs as (Derwent et al., 2010):

$$SOAP_i = \frac{\text{Increment in SOA mass concentration with species}_i}{\text{Increment in SOA with toluene}} \times 100, (9)$$

where SOAP is expressed as an index relative to toluene multiplied by 100. Toluene was chosen as the base compound for the SOAP scale because its emissions are well characterized and it is widely recognized as an important human-made precursor to SOA formation (Hu et al., 2008; Kleindienst et al., 2007). Secondly, to have a direct evaluation of VOCs to SOA, we converted the Toluene-Equivalent SOAP into mass-based values according to toluene gas-to-particle chamber test results under a high nitrogen oxide (NO_x) condition and low temperature (Johnson et al., 2004). The case was chosen because the simulation conditions were similar to those in the Guanzhong Basin in wintertime. Under such conditions, the final gas-to-particle ratio was calculated as 0.045 for toluene (Johnson et al., 2004). The Toluene-Equivalent SOAPs and the gas-to-particle converted SOAP are illustrated in Figure 2.

Insert Figure 2a and 2b

Overall, aromatic hydrocarbons constitute the dominant group for the estimated Toluene-Equivalent SOAP because they demonstrate higher photo-oxidation reactivity than do alkane and alkenes; this is especially true for the highly volatile hydrocarbons that participate in gas-to-particle reactions (Johnson et al., 2004). Followed by aromatic hydrocarbons, alkane was the second largest contributor to Toluene-Equivalent SOAP; this could be explained by the relatively high photo-oxidation reactivity for long-chain alkanes (Derwent et al., 2010). Since alkenes and oxygenated-VOCs (grouped as “Others”) generally have lower toluene-equivalence indexes than aromatic hydrocarbons and alkanes (especially long-chain ones), their contributions to SOAP were low. Similar phenomena were observed for the gas-to-particle transferred SOAP (Figure 2b) with relatively low conversion values.

For biomass fuels, the Toluene-Equivalent SOAPs ranged from 0.24 ± 0.032 to 1.01 ± 0.067 g kg⁻¹, with the highest and lowest SOAP values found for firewood-SG and branch-TS, respectively. Unlike the OFP results, the SOAP values from semi-gasifier emissions were at least double ($p < 0.05$) those from Heated Kang emissions when the same fuel was used. Alkane was the second largest contributor from semi-gasifier and cooking stoves but its contribution was lower than that of alkenes from Heated Kang stoves. The SOAPs of the group of “Others” were negligible because they were 1–2 orders of magnitude lower than those of the major groups ($p < 0.05$). Coal fuels (0.129 ± 0.166 g kg⁻¹) showed over 70% lower average SOAPs than did biomass fuels (0.558 ± 0.315 g kg⁻¹), even though bitumite showed over 30 times higher SOAP than did anthracite and was at the same level with biomass fuels. Specifically, the lowest SOAP of 0.011 ± 0.004 g kg⁻¹ was observed for honeycomb-CS, whereas bitumite-SG had the highest SOAP of 0.365 ± 0.099 g kg⁻¹, even lower than the average value for the biomass burning although the difference was not significant ($p > 0.05$). As previously discussed, the long-chain alkanes and aromatic hydrocarbons are the predominant VOCs in coal combustion

emissions, and they occupied the majority of the SOAPs. The fractions of alkenes and the “Others” group were obviously lower than those of biomass combustion ($p < 0.05$). The mass-based SOAPs ranged from 0.5 ± 0.2 to 45.6 ± 3.0 mg kg⁻¹. Compared with the data in previous studies (Shen et al., 2015; Sun et al., 2017), the current SOAPs were nearly 1,000 times lower than the EFs of primary PM_{2.5}.

To evaluate the SOA contributions from solid fuel burning in the Guanzhong Basin, a rough calculation was done and all parameters and results are listed in Table S9. As depicted in Figure S9, the emission rate of SOAPs from biomass fuels burning (387 kg day⁻¹) was at the same level as that from coal burning (410 kg day⁻¹). The contribution of solid fuel burning to SOA in the Guanzhong Basin was estimated to be 0.23%, which was much lower than the value of 7.6% that had been obtained with a PM_{2.5} source apportionment method (Huang et al., 2014). Thus, the contribution of VOCs to SOA was not comparable to that of the primary PM_{2.5}. Hence, the VOC emissions from solid fuel burning were more significantly causative of the O₃ pollution in the Guanzhong atmosphere. Uncertainties about the SOA contribution evaluation were similar to those regarding the O₃ evaluation.

Insert Table S9

3.5 Uncertainties

Sources and levels of uncertainty throughout the study were calculated using Eqs. (3) to (5). First, uncertainties from VOC analyzing measurements were calculated (Supporting Information 3). On average 86 of 98 VOC species were over the MDL but the uncertainties were high for species with concentrations lower than the MDL. Furthermore, the average level of uncertainty for the VOCs with concentrations over the MDL was 28.7% (from 14.5% to 58.9%), which was reasonable and acceptable relative to the range of SDs (24.2% to 69.4% with average of 45.2%). It also indicates that the uncertainties derived from experimental error in duplication tests were higher than those from VOC measurements.

As shown in Eq. (1), the uncertainties of EFs calculation were affected by many sources. The m_{tube} was found by analyzing results and uncertainties as previously discussed (on average 28.7%). DR and Q_{tube} were measured by TSI 4140 with an uncertainty of 2%; the ruler and balance used in this study both had an uncertainty of 0.1%, and the uncertainty of the timer was negligible. Thus, the average uncertainty level for main EFs was calculated to be 28.8%. As the SDs were shown in the manuscript, the uncertainty level of EFs was 28.8%. This also implies that the main source of uncertainty in EF measurements was from experimental error due to the limited number of samples, and the other sources in sample collection and analysis were comparably low. The profile data of VOCs were based on the EF data but without SD, thus the uncertainty level was combined as 45.3% as well. For OFP and SOAP estimations, the MIR and k_{oh} methods did not refer to the uncertainty level, thus the uncertainty levels in OFP and SOAP calculations were the same as that of the EFs (28.8%).

For the box model, the main sources of uncertainty were EFs, fuel consumption estimation, heating days, and atmospheric capacity (height of boundary layer). The uncertainty level for EFs was set as 28.8%, the variation of heating days was 10%, the uncertainty of average boundary layer height was set

as 30%. For the estimation of total fuel consumption, statistical data and two estimated proportions were used; each of them had an uncertainty level of 20%. As the SD was not calculated in this part, the average SD level was also considered in the uncertainty calculation of the box model. After propagation of all the relative uncertainties, the total uncertainty level of box model results was calculated to be 71.2%. Therefore, the simulated data also had meanings that referred to local O₃ source identification. The largest source of uncertainty in this study was from experimental error (45.2%), indicating that the limited sample number in this study had crucial effects on the uncertainty level. Therefore, a more comprehensive and reasonable investigation of VOC emissions from solid fuel use in the Guanzhong Plain is warranted.

4. Conclusion

Residential solid fuel burning is common for cooking and space heating in the rural Guanzhong Plain, China. Eight types of widely used solid fuels and three types of stoves were selected in this study to detect the VOC emission profiles and their potential influences on ozone and SOA formation. VOC samples were collected on site using a custom-made dilution system set directly on the chimney of each stove. The results of VOC EFs illustrated that biomass straw combustion emitted the most VOCs with EFs of 1.81 ± 0.83 to 3.12 ± 1.59 g kg⁻¹, followed by wood fuels (1.12 ± 0.18 to 2.50 ± 0.73 g kg⁻¹), and coal fuels (0.047 ± 0.019 to 1.00 ± 0.47 g kg⁻¹). Alkanes and aromatic hydrocarbons were the most abundant categories of VOCs emitted from coal burning. For straw and wood fuels, alkenes and carbonyls also contributed considerable proportions to the total VOCs (other than alkanes and aromatic hydrocarbons). Semi-gasifier stoves were proved to be ineffective in decreasing the total VOC emissions for straw and wood combustion when compared to traditional stoves. When using coal fuels, semi-gasifier stoves emitted 10 times more VOCs than did other stoves. CD values between VOC profiles from the same stove type were lower than those from different stove types using the same fuel, and this indicated that collecting VOC profiles by stove type was useful for recording an inventory of sources. Simplified box model results indicated that solid fuel burning related VOCs in the Guanzhong plain contributed approximately 20% to regional O₃ formation in winter, which was much higher than the contribution to SOA formation (only 0.23%). Considering the uncertainty level of the box model, the concentration to SOAP was negligible. Therefore, the limitation of VOC emissions from residential solid fuel burning could be an effective approach to decrease O₃ levels in the Guanzhong Plain, China.

Reference

- Acosta, J.A., Faz, A., Kalbitz, K., Jansen, B., Martinez-Martinez, S., 2011. Heavy metal concentrations in particle size fractions from street dust of Murcia (Spain) as the basis for risk assessment. *Journal of Environmental Monitoring* 13, 3087-3096.
- Adkins, E., Tyler, E., Wang, J., Siriri, D., Modi, V., 2010. Field testing and survey evaluation of household biomass cookstoves in rural sub-Saharan Africa. *Energy for Sustainable Development* 14, 172-185.
- Akagi, S.K., Yokelson, R.J., Wiedinmyer, C., Alvarado, M.J., Reid, J.S., Karl, T., Crounse, J.D., Wennberg, P.O., 2011. Emission factors for open and domestic biomass burning for use in atmospheric models. *Atmospheric Chemistry and Physics* 11, 4039-4072.
- Andreae, M.O., Artaxo, P., Fischer, H., Freitas, S.R., Gregoire, J.M., Hansel, A., Hoor, P., Kormann, R., Krejci, R., Lange, L., Lelieveld, J., Lindinger, W., Longo, K., Peters, W., de Reus, M., Scheeren, B., Dias, M., Strom, J., van Velthoven, P.F.J., Williams, J., 2001. Transport of biomass burning smoke to the upper troposphere by deep convection in the equatorial region. *Geophysical Research Letters* 28, 951-954.
- Atkinson, R., Arey, J., 2003. Atmospheric degradation of volatile organic compounds. *Chemical Reviews* 103, 4605-4638.
- Baxter, L., 2005. Biomass-coal co-combustion: opportunity for affordable renewable energy. *Fuel* 84, 1295-1302.
- Bonjour, S., Adair-Rohani, H., Wolf, J., Bruce, N.G., Mehta, S., Pruess-Ustuen, A., Lahiff, M., Rehfuess, E.A., Mishra, V., Smith, K.R., 2013. Solid Fuel Use for Household Cooking: Country and Regional Estimates for 1980-2010. *Environmental Health Perspectives* 121, 784-790.
- Cao, J.J., Wu, F., Chow, J.C., Lee, S.C., Li, Y., Chen, S.W., An, Z.S., Fung, K.K., Watson, J.G., Zhu, C.S., Liu, S.X., 2005. Characterization and source apportionment of atmospheric organic and elemental carbon during fall and winter of 2003 in Xi'an, China. *Atmospheric Chemistry and Physics* 5, 3127-3137.
- Carter, W.P., 2009. Carter W P L. Updated maximum incremental reactivity scale and hydrocarbon bin reactivities for regulatory applications. California Air Resources Board Contract 2009, 339.
- Carter, W.P., Gookyoung Heo, David R. Cocker III, and Shunsuke Nakao, 2012. SOA Formation: Chamber Study and Model Development[J]. California Air Resources Board 2012, 326.
- Chagger, H.K., Jones, J.M., Pourkashanian, M., Williams, A., Owen, A., Fynes, G., 1999. Emission of volatile organic compounds from coal combustion. *Fuel* 78, 1527-1538.
- Chen, Y., Shen, G., Liu, W., Du, W., Su, S., Duan, Y., Lin, N., Zhuo, S., Wang, X., Xing, B., Tao, S., 2016. Field measurement and estimate of gaseous and particle pollutant emissions from cooking and space heating processes in rural households, northern China. *Atmospheric Environment* 125, 265-271.
- Derwent, R.G., Jenkin, M.E., Utembe, S.R., Shallcross, D.E., Murrells, T.P., Passant, N.R., 2010. Secondary organic aerosol formation from a large number of reactive man-made organic compounds. *Science of the Total Environment* 408, 3374-3381.
- Duan, J., Tan, J., Yang, L., Wu, S., Hao, J., 2008. Concentration, sources and ozone formation potential of volatile organic compounds (VOCs) during ozone episode in Beijing. *Atmospheric Research* 88, 25-35.
- Evtugina, M., Alves, C., Calvo, A., Nunes, T., Tarelho, L., Duarte, M., Prozil, S.O., Evtuguin, D.V., Pio, C., 2014. VOC emissions from residential combustion of Southern and mid-European woods. *Atmospheric Environment* 83, 90-98.
- Ho, K.F., Ho, S.S.H., Lee, S.C., Louie, P.K.K., Cao, J., Deng, W., 2013. Volatile Organic Compounds in Roadside Environment of Hong Kong. *Aerosol and Air Quality Research* 13, 1331-1347.
- Ho, S.S.H., Chow, J.C., Watson, J.G., Wang, L., Qu, L., Dai, W., Huang, Y., Cao, J., 2017. Influences of relative humidities and temperatures on the collection of C-2-C-5 aliphatic hydrocarbons with multi-bed (Tenax TA, Carbograph 1TD, Carboxen 1003) sorbent tube method. *Atmospheric Environment* 151, 45-51.
- Ho, S.S.H., Wang, L., Chow, J.C., Watson, J.G., Xue, Y., Huang, Y., Qu, L., Li, B., Dai, W., Li, L., Cao, J., 2018. Optimization and evaluation of multi-bed adsorbent tube method in collection of volatile organic compounds. *Atmospheric Research* 202, 187-195.
- Hou, B.-D., Tang, X., Ma, C., Liu, L., Wei, Y.-M., Liao, H., 2017. Cooking fuel choice in rural China: results from microdata. *Journal of Cleaner Production* 142, 538-547.
- Hu, D., Bian, Q., Li, T.W.Y., Lau, A.K.H., Yu, J.Z., 2008. Contributions of isoprene, monoterpenes, beta-caryophyllene, and toluene to secondary organic aerosols in Hong Kong during the summer of 2006. *Journal of Geophysical Research-Atmospheres* 113.
- Huang, R.-J., Zhang, Y., Bozzetti, C., Ho, K.-F., Cao, J.-J., Han, Y., Daellenbach, K.R., Slowik, J.G., Platt, S.M., Canonaco, F., Zotter, P., Wolf, R., Pieber, S.M., Brun, E.A., Crippa, M., Ciarelli, G.,

524 Piazzalunga, A., Schwikowski, M., Abbaszade, G., Schnelle-Kreis, J., Zimmermann, R., An, Z., Szidat,
 525 S., Baltensperger, U., El Haddad, I., Prevot, A.S.H., 2014. High secondary aerosol contribution to
 526 particulate pollution during haze events in China. *Nature* 514, 218-222.
 527 Hwa, M.-Y., Hsieh, C.-C., Wu, T.-C., Chang, L.-F.W., 2002. Real-world vehicle emissions and VOCs
 528 profile in the Taipei tunnel located at Taiwan Taipei area. *Atmospheric Environment* 36, 1993-2002.
 529 Iinuma, Y., Boege, O., Graefe, R., Herrmann, H., 2010. Methyl-Nitrocatechols: Atmospheric Tracer
 530 Compounds for Biomass Burning Secondary Organic Aerosols. *Environmental Science & Technology*
 531 44, 8453-8459.
 532 Johnson, D., Jenkin, M.E., Wirtz, K., Martin-Reviejo, M., 2004. Simulating the Formation of
 533 Secondary Organic Aerosol from the Photooxidation of Toluene. *Environmental Chemistry* 1, 150-165.
 534 Kleindienst, T.E., Jaoui, M., Lewandowski, M., Offenberg, J.H., Lewis, C.W., Bhawe, P.V., Edney, E.O.,
 535 2007. Estimates of the contributions of biogenic and anthropogenic hydrocarbons to secondary organic
 536 aerosol at a southeastern US location. *Atmospheric Environment* 41, 8288-8300.
 537 Langmann, B., Duncan, B., Textor, C., Trentmann, J., van der Werf, G.R., 2009. Vegetation fire
 538 emissions and their impact on air pollution and climate. *Atmospheric Environment* 43, 107-116.
 539 Lee, S., Baumann, K., Schauer, J.J., Sheesley, R.J., Naeher, L.P., Meinardi, S., Blake, D.R., Edgerton,
 540 E.S., Russell, A.G., Clements, M., 2005. Gaseous and particulate emissions from prescribed burning in
 541 Georgia. *Environmental Science & Technology* 39, 9049-9056.
 542 Lei, Y., Zhang, Q., He, K.B., Streets, D.G., 2011. Primary anthropogenic aerosol emission trends for
 543 China, 1990-2005. *Atmospheric Chemistry and Physics* 11, 931-954.
 544 Lemieux, P.M., Lutes, C.C., Santoianni, D.A., 2004. Emissions of organic air toxics from open burning:
 545 a comprehensive review. *Progress in Energy and Combustion Science* 30, 1-32.
 546 Li, B., Ho, S.S.H., Xue, Y., Huang, Y., Wang, L., Cheng, Y., Dai, W., Zhong, H., Cao, J., Lee, S., 2017.
 547 Characterizations of volatile organic compounds (VOCs) from vehicular emissions at roadside
 548 environment: The first comprehensive study in Northwestern China. *Atmospheric Environment* 161,
 549 1-12.
 550 Li, X., Wang, S., Duan, L., Hao, J., 2009. Characterization of non-methane hydrocarbons emitted from
 551 open burning of wheat straw and corn stover in China. *Environmental Research Letters* 4.
 552 Lindberg, D., Niemi, J., Engblom, M., Yrjas, P., Lauren, T., Hupa, M., 2016. Effect of temperature
 553 gradient on composition and morphology of synthetic chlorine-containing biomass boiler deposits. *Fuel*
 554 Processing Technology 141, 285-298.
 555 Liu, C., Zhang, C., Mu, Y., Liu, J., Zhang, Y., 2017. Emission of volatile organic compounds from
 556 domestic coal stove with the actual alternation of flaming and smoldering combustion processes.
 557 *Environmental Pollution* 221, 385-391.
 558 Liu, Y., Shao, M., Fu, L., Lu, S., Zeng, L., Tang, D., 2008. Source profiles of volatile organic
 559 compounds (VOCs) measured in China: Part I. *Atmospheric Environment* 42, 6247-6260.
 560 Niu, X., Cao, J., Shen, Z., Ho, S.S.H., Tie, X., Zhao, S., Xu, H., Zhang, B., Huang, R., 2016. PM_{2.5}
 561 from the Guanzhong Plain: Chemical composition and implications for emission reductions.
 562 *Atmospheric Environment* 147, 458-469.
 563 Reid, J.S., Koppmann, R., Eck, T.F., Eleuterio, D.P., 2005. A review of biomass burning emissions part
 564 II: intensive physical properties of biomass burning particles. *Atmospheric Chemistry and Physics* 5,
 565 799-825.
 566 Shen, G., Chen, Y., Xue, C., Lin, N., Huang, Y., Shen, H., Wang, Y., Li, T., Zhang, Y., Su, S., Huangfu,
 567 Y., Zhang, W., Chen, X., Liu, G., Liu, W., Wang, X., Wong, M.-H., Tao, S., 2015. Pollutant Emissions
 568 from Improved Coal- and Wood-Fuelled Cookstoves in Rural Households. *Environmental Science &*
 569 *Technology* 49, 6590-6598.
 570 Shen, G., Tao, S., Chen, Y., Zhang, Y., Wei, S., Xue, M., Wang, B., Wang, R., Lu, Y., Li, W., Shen, H.,
 571 Huang, Y., Chen, H., 2013. Emission Characteristics for Polycyclic Aromatic Hydrocarbons from Solid
 572 Fuels Burned in Domestic Stoves in Rural China. *Environmental Science & Technology* 47,
 573 14485-14494.
 574 Shen, Z., Cao, J., Arimoto, R., Han, Z., Zhang, R., Han, Y., Liu, S., Okuda, T., Nakao, S., Tanaka, S.,
 575 2009. Ionic composition of TSP and PM_{2.5} during dust storms and air pollution episodes at Xi'an,
 576 China. *Atmospheric Environment* 43, 2911-2918.
 577 Sun, J., Shen, Z., Cao, J., Zhang, L., Wu, T., Zhang, Q., Yin, X., Lei, Y., Huang, Y., Huang, R.J., Liu, S.,
 578 Han, Y., Xu, H., Zheng, C., Liu, P., 2017. Particulate matters emitted from maize straw burning for
 579 winter heating in rural areas in Guanzhong Plain, China: Current emission and future reduction.
 580 *Atmospheric Research* 184, 66-76.
 581 Tie, X., Zhang, Q., He, H., Cao, J., Han, S., Gao, Y., Li, X., Jia, X.C., 2015. A budget analysis of the
 582 formation of haze in Beijing. *Atmospheric Environment* 100, 25-36.
 583 Vassilev, S.V., Eskenazy, G.M., Vassileva, C.G., 2000. Contents, modes of occurrence and origin of

chlorine and bromine in coal. *Fuel* 79, 903-921.

Wang, H., Lou, S., Huang, C., Qiao, L., Tang, X., Chen, C., Zeng, L., Wang, Q., Zhou, M., Lu, S., Yu, X., 2014. Source Profiles of Volatile Organic Compounds from Biomass Burning in Yangtze River Delta, China. *Aerosol and Air Quality Research* 14, 818-828.

Wang, T., Xue, L., Brimblecombe, P., Lam, Y.F., Li, L., Zhang, L., 2017. Ozone pollution in China: A review of concentrations, meteorological influences, chemical precursors, and effects. *Science of the Total Environment* 575, 1582-1596.

Westberg, H.M., Bystrom, M., Leckner, B., 2003. Distribution of potassium, chlorine, and sulfur between solid and vapor phases during combustion of wood chips and coal. *Energy & Fuels* 17, 18-28.

Winijkul, E., Bond, T.C., 2016. Emissions from residential combustion considering end-uses and spatial constraints: Part II, emission reduction scenarios. *Atmospheric Environment* 124, 1-11.

Xue, Y., Ho, S.S.H., Huang, Y., Li, B., Wang, L., Dai, W., Cao, J., Lee, S., 2017. Source apportionment of VOCs and their impacts on surface ozone in an industry city of Baoji, Northwestern China. *Scientific Reports* 7, 9979.

Yuan, B., Liu, Y., Shao, M., Lu, S., Streets, D.G., 2010. Biomass Burning Contributions to Ambient VOCs Species at a Receptor Site in the Pearl River Delta (PRD), China. *Environmental Science & Technology* 44, 4577-4582.

Yudovich, Y.E., Ketris, M.P., 2006. Chlorine in coal: A review. *International Journal of Coal Geology* 67, 127-144.

Zhang, J.J., Smith, K.R., 2007. Household air pollution from coal and biomass fuels in China: Measurements, health impacts, and interventions. *Environmental Health Perspectives* 115, 848-855.

Zhang, Q., Shen, Z., Cao, J., Zhang, R., Zhang, L., Huang, R.J., Zheng, C., Wang, L., Liu, S., Xu, H., Zheng, C., Liu, P., 2015. Variations in PM_{2.5}, TSP, BC, and trace gases (NO₂, SO₂, and O₃) between haze and non-haze episodes in winter over Xi'an, China. *Atmospheric Environment* 112, 64-71.

Zhuang, Z., Li, Y., Chen, B., Guo, J., 2009. Chinese kang as a domestic heating system in rural northern China-A review. *Energy and Buildings* 41, 111-119.

612 **Figure Legends**

613 **Figure 1** EFs of MIR-OFP (a) and propane-equivalent (b) emitted from residential heating and cooking
614 activities

615 **Figure 2** EFs of SOAP (Toluene-equivalent) (a) and SOAP (Gas to Particle transfer rate) (b) emitted
616 from residential heating and cooking activities

617

618 **Supporting Information (SI)**

619 (1) SI1: Raw data of manuscript. (2) SI2: Detailed information on results and discussions: Figure
620 S1-S3 and Table S1-S9. (3) SI3 Results of uncertainties

621

622

623 Table 1 EFs of eight classes of VOCs emitted from residential heating and cooking activities (g·kg⁻¹)

| | Wood heating | | | | Straw heating | | Coal heating | | | Cooking | | |
|------------------------------|------------------|-------------------|---------------------|-----------------|-----------------|-------------|------------------------|---------------------|--------------|---------------------|-------------|-----------------|
| | Heated Kang | | Semi-gasifier stove | | Heated Kang | | Traditional coal stove | Semi-gasifier stove | Bitumit | Old fashioned stove | | |
| | Firewood | Branch | Firewood | Branch | Maize straw | Wheat straw | Anthracite | Honey-comb | Anthracite | e | Branch | Corncob |
| Alkanes | 0.712±0.20 4 | 0.519±0.06 1 | 0.716±0.265 | 0.629±0.38 4 | 0.638±0.2 99 | 0.409±0.220 | 0.035±0.011 | 0.021±0.0 12 | 0.228±0.132 | 0.450±0.2 94 | 0.331±0.091 | 0.812±0.74 4 |
| Alkenes | 0.516±0.14 1 | 0.32±0.071 | 0.26±0.11 | 0.13±0.06 | 0.41±0.15 | 0.030±0.014 | 0.003±0.001 | 0.001±0.0 05 | 0.014.9±0.00 | 0.066±0.0 33 | 0.059±0.012 | 0.146±0.16 1 |
| Aromatic hydrocarbons | 0.404±0.02 5 | 0.41±0.12 | 1.14±0.26 | 0.92±0.16 | 0.32±0.22 | 0.36±0.15 | 0.013±0.002 | 0.011±0.0 03 | 0.18±0.039 | 0.038±0.0 12 | 0.264±0.037 | 1.12±0.54 |
| Carbonyls | 0.712±0.12 1 | 0.52±0.06 | 0.26±0.039 | 0.45±0.14 | 0.68±0.15 | 0.53±0.25 | 0.006±0.002 | 0.003±0.0 01 | 0.048±0.022 | 0.019±0.0 03 | 0.196±0.009 | 0.64±0.061 |
| Alcohols | 0.0007±0 002 | 0.0005±0.0 002 | 0.009±0.009 | 0.11±0.03 | 0.02±0.00 3 | 0.099±0.054 | 0.006±0.002 | 0.0017±0. 0001 | 0.031±0.012 | 0.020±0.0 02 | 0.061±0.014 | 0.033±0.00 4 |
| Esters | 0.007±0.00 07 | 0.006±0.00 1 | 0.009±0.006 | 0.013±0.00 6 | 0.007±0.0 04 | 0.026±0.012 | 0.003±0.0003 | 0.002±0.0 005 | 0.010±0.004 | 0.007±0.0 01 | 0.025±0.003 | 0.031±0.00 8 |
| Halogen-containing compounds | 0.045±0.00 5 | 0.040±0.01 2 | 0.10±0.03 | 0.12±0.03 | 0.093±0.0 23 | 0.31±0.13 | 0.011±0.002 | 0.008±0.0 02 | 0.066±0.023 | 0.050±0.0 15 | 0.173±0.012 | 0.321±0.07 3 |
| Others | 0.029±0.00 3 | 0.016±0.00 4 | 0.007±0.006 | 0.006±0.00 4 | 0.016±0.0 08 | 0.056±0.008 | 0.001±0.0002 | 0.0002±0. 0001 | 0.017±0.009 | 0.003±0.0 02 | 0.011±0.001 | 0.020±0.00 1 |
| Total | 2.43±0.50 | 1.83±0.33 | 2.50±0.73 | 2.37±0.82 | 2.18±0.86 | 1.8±0.83 | 0.078±0.019 | 0.047±0.0 19 | 0.599±0.25 | 1.00±0.47 | 1.12±0.18 | 3.12±1.59 |

624

625 Table 2 Contributions of the top ten VOC to the EFs in each test

| Firewood-HK | EFs | Branch-HK | EFs | Firewood-SG | EFs | Branch-SG | EFs |
|---------------------|-------|---------------------|-------|---------------------|-------|---------------------|-------|
| iso-Pentane | 14.8% | iso-Pentane | 13.5% | Benzene | 16.5% | Benzene | 17.1% |
| Acetone | 14.5% | Acetone | 13.2% | Toluene | 11.0% | Acetone | 10.6% |
| Propylene | 12.1% | Benzene | 10.3% | Acetone | 6.6% | iso-Pentane | 7.4% |
| Methyl ethyl ketone | 7.4% | Propylene | 10.2% | Propylene | 6.5% | Naphthalene | 6.1% |
| Acrolein | 7.0% | Methyl ethyl ketone | 8.1% | Dodecane | 6.2% | Toluene | 5.3% |
| Propane | 6.9% | Acrolein | 5.9% | iso-Pentane | 4.4% | Dodecane | 5.0% |
| Benzene | 6.8% | Toluene | 5.8% | Naphthalene | 4.2% | Acrolein | 4.9% |
| Toluene | 4.3% | Propane | 5.5% | Propane | 4.2% | Ethanol | 4.3% |
| 1,3-Butadiene | 2.4% | 1,3-Butadiene | 2.4% | p-Xylene | 2.5% | Methyl ethyl ketone | 3.3% |
| 1-Butene | 2.0% | 2-Methylpentane | 2.2% | m-Xylene | 2.5% | Propane | 2.7% |
| Maize-HK | EFs | Wheat-HK | EFs | Branch-TS | EFs | Corn cob-TS | EFs |
| Acetone | 17.5% | Acetone | 13.2% | Benzene | 10.6% | Benzene | 14.4% |
| iso-Pentane | 15.6% | Methyl ethyl ketone | 8.1% | Acetone | 8.4% | Dodecane | 11.6% |
| Propylene | 12.5% | iso-Pentane | 7.3% | iso-Pentane | 8.2% | Naphthalene | 8.6% |
| Methyl ethyl ketone | 8.8% | Chloromethane | 5.3% | Dodecane | 5.6% | Acetone | 7.3% |
| Benzene | 6.4% | Acrolein | 5.0% | Ethanol | 5.1% | Acrolein | 7.1% |
| Propane | 6.3% | Ethanol | 4.9% | Acrolein | 4.1% | iso-Pentane | 5.7% |
| Toluene | 4.7% | Toluene | 4.6% | Toluene | 4.0% | Methyl ethyl ketone | 4.9% |
| Acrolein | 4.4% | Benzene | 3.8% | Methyl ethyl ketone | 4.0% | Toluene | 4.5% |
| 1-Butene | 2.0% | 1,3-Butadiene | 3.5% | n-Butane | 3.7% | 1,4-Dichlorobenzene | 4.2% |
| Chloromethane | 2.0% | Propane | 3.4% | Naphthalene | 3.4% | 1,3-Butadiene | 2.8% |
| Anthracite-CS | EFs | Honeycomb-CS | EFs | Anthracite-SG | | Bitumite-SG | EFs |
| Dodecane | 17.1% | Dodecane | 21.3% | Dodecane | 21.2% | Benzene | 12.1% |
| n-Butane | 9.5% | n-Butane | 7.9% | Naphthalene | 15.2% | Dodecane | 10.5% |
| Ethanol | 7.6% | Naphthalene | 6.6% | Acetone | 5.5% | Toluene | 8.4% |
| iso-Pentane | 6.5% | Benzene | 5.9% | Ethanol | 5.0% | n-Butane | 7.8% |

| | | | | | | | |
|---------------------|------|---------------------|------|---------------------|------|-------------|------|
| Benzene | 4.3% | 1,4-Dichlorobenzene | 4.3% | Benzene | 4.6% | Undecane | 5.3% |
| Naphthalene | 3.8% | Toluene | 3.7% | n-Butane | 3.7% | Isobutane | 5.3% |
| Methyl ethyl ketone | 3.5% | Ethanol | 3.3% | Toluene | 3.6% | Naphthalene | 4.7% |
| 1,4-Dichlorobenzene | 3.1% | Methyl ethyl ketone | 2.9% | 1,4-Dichlorobenzene | 2.7% | Propane | 3.9% |
| Toluene | 3.1% | 1,3-Dichlorobenzene | 2.8% | Isobutane | 2.4% | iso-Pentane | 2.6% |
| Acetone | 2.6% | Ethyl Acetate | 2.4% | Undecane | 2.1% | n-Pentane | 2.2% |

*Top ten species were selected according to majority of results. The cumulative frequency of top ten species was over 60%, which were sufficiently representative to each test.

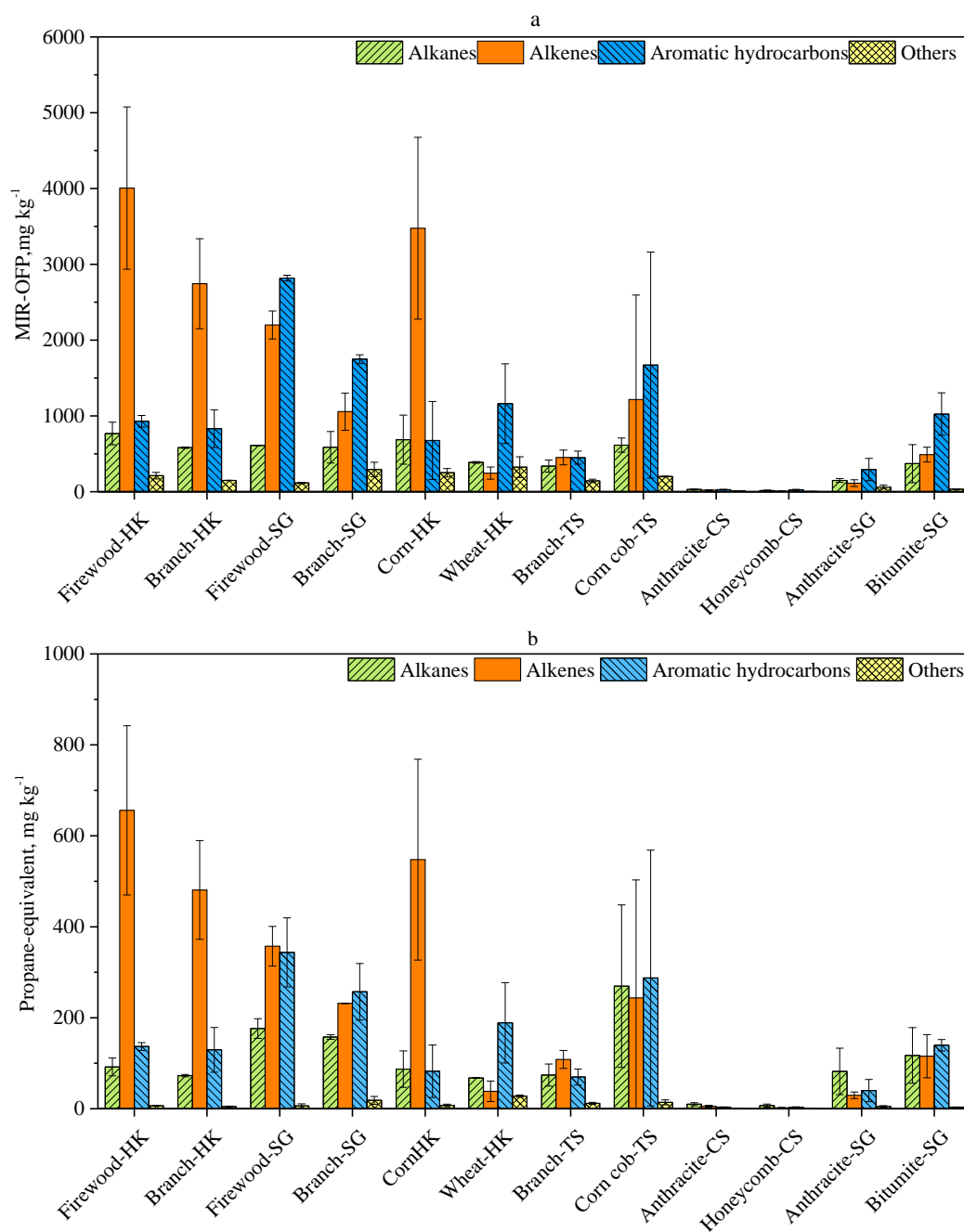


Figure 1. EFs of MIR-OFP (a) and propane-equivalent (b) emitted from residential heating and cooking activities

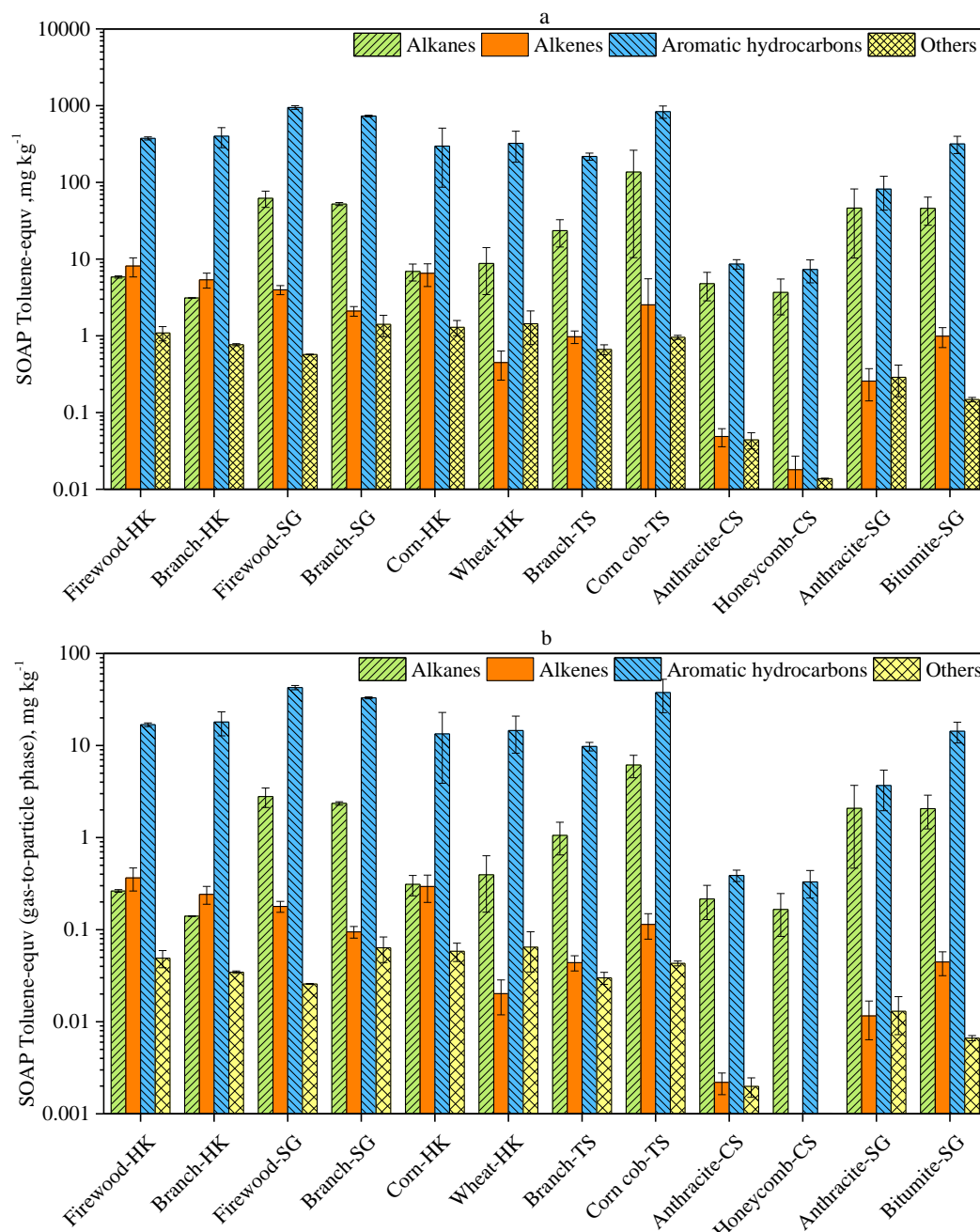


Figure 2 EFs of SOAP (Toluene-equivalent) (a) and SOAP (Gas to Particle transfer rate) (b) emitted from residential heating and cooking activities